Modeling of Magnetization Dynamics Using Saturation Wavefronts

Martin Petrun[1], S. Steentjes[2], K. Hameyer[2], and D. Dolinar[1]

[1]Institute of Power Engineering, FERI, University of Maribor, 2000 Maribor, Slovenia
[2]Institute of Electrical Machines, RWTH Aachen University, 52062 Aachen, Germany

This paper presents a detailed theoretical background of the saturation wave model (SWM), which offers a simplified homogenized solution of the nonlinear diffusion phenomena inside soft magnetic steel sheets (SMSSs). The SWM is capable of predicting the complicated dynamic magnetization of SMSS without discretization of the cross section of the SMSSs. Despite its simplicity, the SWM predicts exact solutions of the discussed problems when step-like magnetization curves are assumed and reasonably accurate solutions for real magnetization curves. In this paper, the SWM is analyzed in comparison to the numerical solution of the diffusion phenomena using the parametric magnetodynamic model, where interesting properties of the SWM are discussed and pointed out.

***Index Terms*— Eddy current diffusion, magnetic hysteresis, magnetic power loss, saturation wave model (SWM), soft magnetic materials.**

I. Introduction

MAGNETIZATION dynamics and iron losses in soft magnetic steel sheets (SMSSs) are a result of the intricate coupling of eddy currents and static hysteresis [1]. Nowadays, the phenomena is usually described using a 1-D approximation and can be solved by discretization of SMSSs in different ways [2]. In addition to a proper modeling at the level of individual laminations, resolving small-scale interactions between eddy currents and hysteresis requires a numerical, in most cases iterative, time-stepping procedure. The obtained models can be very complex, despite a number of simplifying assumptions. Direct incorporation of the 1-D diffusion equation into 2-D finite element analysis of electrical machines is hence rather technical and cumbersome and makes it necessary to significantly modify the finite element code.

A substantial simplification of the problem can be achieved if homogenized models are applied, which describe the magnetization behavior averaged over the cross section. For some applications, sufficiently accurate solutions can be achieved using several versions of the thin sheet model (TSM) [3]–[5]. As an alternative to TSMs, the saturation wave model (SWM) can be applied, which improves the description of classical eddy currents [6]–[8].

Several works show that the SWM performs surprisingly well under different excitation conditions, despite its simplicity [3], [6], [7]. Most papers, however, extend the classical SWM to include additional magnetic field components, e.g., to accommodate the excess phenomena [$H_{\mathrm{exc}}(t)$]. By addition of such terms, the deficiencies of the SWM eddy current term are compensated as well. This is why this paper aims at analyzing only the eddy current term of the SWM. For this purpose, the SWM is compared with the established and more complex parametric magnetodynamic (PMD) model [9], [10] that solves the 1-D diffusion problem using spatial discretization of the SMSS. In this way, the ability of the simplified homogenized SWM to reproduce the dynamic hysteresis loop shapes and iron losses will be studied.

Manuscript received August 10, 2016; revised September 20, 2016; accepted October 10, 2016. Date of publication October 19, 2016; date of current version March 16, 2017. Corresponding author: M. Petrun (e-mail: martin.petrun@um.si).

Color versions of one or more of the figures in this paper are available online at http://ieeexplore.ieee.org.

Digital Object Identifier 10.1109/TMAG.2016.2618947

II. Simplified Models of Laminations

Simplified solutions that take into account the whole cross section without discretization are in general hampered by the magnetic-field-dependent differential permeability and consequent nonlinear skin effect [11]. The discussed problem can be, in general, solved by assuming one of the two crude approximations.

The first approximation takes integral impact of induced eddy currents on the magnetic field. Consequently, it links $H(t)$ at the sheet surface and the average value $B_{\mathrm{a}}(t)$ over the cross section of the SMSS. The representative of this group is the TSM [3]–[5]. The deficiency and limitation of such an approximation is obvious; such a simplified model cannot take the skin effect into account. Therefore, it is limited to low excitation dynamics where the skin effect is negligible [4].

The second approximation is the solution of the 1-D problem assuming a constant permeability. Such an approximation appears even more unnatural at first glance, as the linear skin effect can differ substantially in comparison to its nonlinear counterpart [11], [12]. Especially a big impact on the skin effect has the saturation region with its flat $B(H)$ curve [11]. Therefore, it is virtually impossible to substitute the highly nonlinear magnetization curve with an equivalent constant permeability. However, despite severe limitations, such models can be applied at some specific conditions, e.g., at very low magnetic fields far from the saturation region [11], [12].

The second approximation can be, however, extended to a special limiting case. As the saturation plays such an important role in the distribution of the magnetic field and eddy currents, it would be convenient to apply a constant differential permeability that is adjusted only for the saturation region. In addition that the differential permeability in this region is in fact constant, its value is very close to zero. Hence,

the differential permeability in the saturation region can be set to zero without oversimplification. However, the problem of the steep nonsaturated curve between both the saturation regions still remains. This problem can be effectively tackled by inserting a finite instantaneous jump between the saturation regions. In this way, a steplike magnetization curve or hysteresis is obtained that enables to solve the discussed problem in an easy and straightforward alternative way in the framework of the SWM. Such a solution was originally proposed in [8] and was further developed in [6], [7], and [12].

A. Saturation Wave Model

If the magnetic material is approximated using a steplike magnetization curve, the magnetic flux density changes instantaneously from B_s to $-B_\mathrm{s}$ when the surface magnetic field strength H_s changes from positive to negative values (and vice versa). In the case that the specific conductivity is zero, $\sigma = 0$, there would be no eddy currents $i_\mathrm{ec}(t)$ and $B(t)$ would change inside the whole SMSS simultaneously. However, due to induced $i_\mathrm{ec}(t)$ that affect $H(t)$, such an instantaneous jump occurs only on the surface of the SMSS. $B(t)$ inside the SMSS changes gradually with time from the surface ($x = 0$) to the middle of the SMSS ($x = b/2$), where b represents the thickness of the SMSS. In this way, a wavefront of amplitude $2B_\mathrm{s}$ is generated. This wavefront propagates from the surface of the SMSS with limited speed $v(t)$. The propagation of the wavefront induces in the SMSS the electric field strength $E(t)$, which can be calculated as

$$E(t) = -2\,B_\mathrm{s}\,\delta\,v(t) = -2\,B_\mathrm{s}\,\delta\,\frac{\mathrm{d}x(t)}{\mathrm{d}t} \tag{1}$$

where δ is a control variable as the sign of the induced $E(t)$ depends on the wavefront character. If the penetrating wavefront is positive, the average magnetic flux density $B_\mathrm{a}(t)$ in the SMSS increases $\left(\frac{\mathrm{d}B_\mathrm{a}}{\mathrm{d}t} > 0\right)$, when the propagating wavefront is negative, $B_\mathrm{a}(t)$ decreases $\left(\frac{\mathrm{d}B_\mathrm{a}}{\mathrm{d}t} < 0\right)$. Induced $E(t)$ generates an eddy current density $j_\mathrm{ec}(t)$ according to the electrical conductivity σ of the SMSS and (1):

$$j_\mathrm{ec}(t) = E(t)\,\sigma = -2\,B_\mathrm{s}\,\delta\,\sigma\,\frac{\mathrm{d}x(t)}{\mathrm{d}t}. \tag{2}$$

The induced eddy current density generates the magnetic field strength $H_\mathrm{ec}(t)$ and has thus a feedback influence on the penetration speed of the saturation wavefront. The resulting magnetic field strength due to eddy currents $H_\mathrm{ec}(t)$ when the wavefront is at position x is given as

$$H_\mathrm{ec}(t) = \frac{i_\mathrm{ec}(t)}{l} = \frac{j_\mathrm{ec}(t)\,l\,x}{l} = -2\,B_\mathrm{s}\,\delta\,\sigma\,x\,\frac{\mathrm{d}x(t)}{\mathrm{d}t} \tag{3}$$

where l is the length of the SMSS and x is the distance of the wavefront from the SMSS's surface.

Along with the penetration of the wavefront, the average flux $\Phi(t)$ and magnetic flux density $B_\mathrm{a}(t)$ inside the SMSS are changing. For example, starting with a negatively saturated SMSS [$\Phi(0) = -\Phi_\mathrm{s}$], the flux $\Phi(t)$ will increase depending on the wavefront position x according to

$$\Phi(t) = \Phi(0) + 2\,\Phi_\mathrm{s}\frac{2x}{b} = -\Phi_\mathrm{s} + 2\,\Phi_\mathrm{s}\frac{2x}{b}. \tag{4}$$

When wavefronts on both the sides are at the surface ($x = 0$), the flux is $\Phi = -\Phi_\mathrm{s}$. Flux $\Phi(t) = 0$, when the wavefronts are at $x = b/4$, as in half of the SMSS positive Φ_s compensates the negative flux $-\Phi_\mathrm{s}$ in the other half of the thickness. On the other side, when both the wavefronts meet at the middle of the SMSS ($x = b/2$), the SMSS is fully saturated in the positive direction and the flux is $\Phi(t) = \Phi_\mathrm{s}$. In the case the excitation magnetization dynamic dictates a magnetic field reversal after positive saturation, a new (negative) wavefront starts to penetrate from the surface of the SMSS. In this case the initial flux is $\Phi(0) = \Phi_\mathrm{s}$. A negative wavefront of amplitude $-2\,\Phi_\mathrm{s}$ decreases $\Phi(t)$ according to

$$\Phi(t) = \Phi(0) - 2\,\Phi_\mathrm{s}\frac{2x}{b} = \Phi_\mathrm{s} - 2\,\Phi_\mathrm{s}\frac{2x}{b}. \tag{5}$$

Equations (4) and (5) are very useful since they link the position x of both the wavefronts with the average flux $\Phi(t)$ inside the SMSS. Therefore, the position x is determined by the following when the average flux $\Phi(t)$ or average magnetic field density $B_a(t)$ are known, respectively:

$$x(t) = \frac{b}{4}\frac{\Phi(t) - \Phi(0)}{\Phi_\mathrm{s}} = \frac{b}{4}\frac{B_\mathrm{a}(t) - B(0)}{B_\mathrm{s}};\quad \frac{\mathrm{d}B_\mathrm{a}(t)}{\mathrm{d}t} > 0 \tag{6}$$

$$x(t) = -\frac{b}{4}\frac{\Phi(t) - \Phi(0)}{\Phi_\mathrm{s}} = -\frac{b}{4}\frac{B_\mathrm{a}(t) - B(0)}{B_\mathrm{s}};\quad \frac{\mathrm{d}B_\mathrm{a}(t)}{\mathrm{d}t} < 0. \tag{7}$$

Using time derivations of (6) and (7), the speed of the wavefronts is obtained by the following, respectively, as:

$$v(t) = \frac{\mathrm{d}x(t)}{\mathrm{d}t} = \frac{b}{4\,B_\mathrm{s}}\frac{\mathrm{d}B_\mathrm{a}(t)}{\mathrm{d}t};\quad \frac{\mathrm{d}B_\mathrm{a}(t)}{\mathrm{d}t} > 0 \tag{8}$$

$$v(t) = \frac{\mathrm{d}x(t)}{\mathrm{d}t} = -\frac{b}{4\,B_\mathrm{s}}\frac{rmdB_\mathrm{a}(t)}{\mathrm{d}t};\quad \frac{\mathrm{d}B_\mathrm{a}(t)}{\mathrm{d}t} < 0. \tag{9}$$

It is important to highlight some properties of the wavefront position x and speed v that are described by (6)–(9). $B_\mathrm{a}(t) = B(0)$ at any reversal point [when the sign of $\left(\frac{\mathrm{d}B_\mathrm{a}}{\mathrm{d}t}\right)$ changes], therefore a new wavefront always starts at the surface ($x = 0$), regardless of whether the generated wavefront is positive or negative. Furthermore, the distance from the surface and the speed of the wavefront is always positive, regardless of whether the average magnetic field density is increasing $\left(\frac{\mathrm{d}B_\mathrm{a}}{\mathrm{d}t} > 0\right)$ or decreasing $\left(\frac{\mathrm{d}B_\mathrm{a}}{\mathrm{d}t} < 0\right)$, whereas $0 \le x \le \left(\frac{b}{2}\right)$.

Based on the determined position and speed of the wavefronts, finally the magnetic field strength due to induced eddy currents $H_\mathrm{ec}(t)$ is determined by inserting (6)–(9) into (3). As the products of (6) and (8) as well as (7) and (9) yield the same results, $H_\mathrm{ec}(t)$ is determined as

$$H_\mathrm{ec}(t) = -\delta\,\frac{\sigma\,b^2}{8}\left(\frac{B_\mathrm{a}(t) - B(0)}{B_\mathrm{s}}\right)\frac{\mathrm{d}B_\mathrm{a}(t)}{\mathrm{d}t}. \tag{10}$$

The magnetic field strength H_s is equal to the magnetic field strength H_stat due to the static magnetization characteristic attenuated by the magnetic field strength due to induced eddy currents H_ec.

$$\begin{aligned} H_\mathrm{s}(t) &= H_\mathrm{stat}(t) - H_\mathrm{ec}(t) \\ &= H_\mathrm{stat}(t) + \delta\,\frac{\sigma\,b^2}{8}\left(\frac{B_\mathrm{a}(t) - B(0)}{B_\mathrm{s}}\right)\frac{\mathrm{d}B_\mathrm{a}(t)}{\mathrm{d}t}. \end{aligned} \tag{11}$$

The SWM is fully described by (11), where (11) is also applicable when the reversal of the magnetic field strength occurs at $|B_a(t)| = |B_T| < |B_s|$. In this case, the magnetization reversal occurs before the wavefront reaches the middle of the SMSS. Immediately after the reversal a new wavefront starts to penetrate from the surface SMSS. In such a case $B_a(t)$ continues at the value of the reversal point, i.e., $B_a(t) = B(0) = B_T$, and starts to increase or decrease according to the excitation.

Using the sign properties of (6) and (7), the SWM (11) can be modified to avoid the control variable δ by introducing the modulus as

$$H_s = H_{stat}(t) + \frac{\sigma b^2}{8} \frac{|B_a(t) - B(0)|}{B_s} \frac{dB_a(t)}{dt}. \quad (12)$$

III. Results

The SWM and the PMD model were both implemented using the commercial MATLAB/Simulink software package. Both the models were analyzed using a quasi steplike as well as real measured magnetization curve. The analysis was performed for a 0.5-mm thick nonoriented steel grade *M400-50A* with a measured specific conductivity $\sigma = 2.16\times10^6 \left(\frac{S}{m}\right)$.

As the PMD calculates the distribution of the magnetic field inside SMSS based on the inverse hysteresis models or magnetization curves $H(B)$, the applied magnetization curve has to be defined for all values of the input variable $B(t)$. This condition is naturally met when applying real magnetization curves. However, by applying an ideal steplike magnetization curve output, $H(t)$ is defined only between $-B_s$ and B_s ($H = 0$). Outside this region H is not defined, therefore the PMD model cannot be solved. To avoid the discussed problem, the saturation regions of the ideal steplike magnetization curve were approximated using a finite slope that was conveniently selected as $\frac{1}{\mu_0}$. The infinitely flat region between $-B_s$ and B_s does not present a problem and was taken into account using a dead zone ($H = 0$). The same quasi steplike magnetization curve was applied also for the static part of the SWM.

Using the PMD model, flux distributions inside an SMSS for different operating conditions were calculated. Based on these calculations average change rates $\left(\frac{dB_a(t)}{dt}\right)$ of magnetic flux density inside the observed SMSS were calculated. These were furthermore used to calculate the prediction of the dynamic term of the SWM.

Fig. 1 shows a comparison of dynamic hysteresis loops under sinusoidal excitation of frequency $f = 1000$ Hz for maximum average magnetic flux densities of $B_{max} = 1.5$ T, $B_{max} = 1.0$ T, and $B_{max} = 0.5$ T, respectively.

The obtained results show excellent agreement between both the discussed models for the major loop as well as for the symmetric minor loops when steplike magnetization curve is used [Fig. 1(a)]. It is, however, worthwhile to note that in this case the PMD model requires a very fine discretization. The magnetic field inside individual slices of the PMD model changes rapidly (Fig. 2), which causes a nonsmooth dynamic curve if the discretization is too coarse. For the presented results $N_s = 160$ slices were applied.

Such excellent agreement, however, deteriorates when the magnetization curve deviates from the ideal steplike curve.

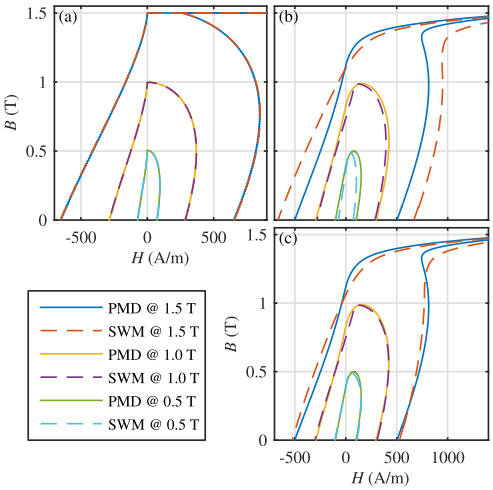

Fig. 1. Comparison of dynamic hysteresis loops using sinusoidal excitation of frequency $f = 1000$ Hz for maximum average flux densities of $B_{max} = 1.5$ T, $B_{max} = 1.0$ T, and $B_{max} = 0.5$ T. (a) Steplike magnetization curve. (b) *M400-50A* nonlinear magnetization curve and $B_s = 1.0$ T. (c) *M400-50A* nonlinear magnetization curve and adjusted B_s.

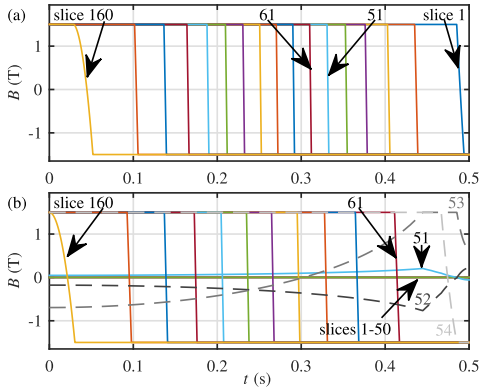

Fig. 2. Calculated magnetic flux densities in different slices of the PMD model for a quarter period of frequency $f = 1000$ Hz for maximum average flux densities of (a) $B_{max} = 1.5$ T and (b) $B_{max} = 1.0$ T.

By applying the *M400-50A* nonlinear magnetization curve to both the models, prediction of the eddy current term of the SWM starts to deviate from the PMD model [Fig. 1(b)]. Despite the increased deviation of the SWM predictions, these agree with the results of the PMD model reasonably well in a broad range of excitation dynamics. Furthermore, it was observed that the deviation between the discussed models depends on the value of B_{max} [Fig. 1(b)]. The predicted loop of the SWM at $B_{max} = 1.5$ T was overestimated, whereas the predicted loop at $B_{max} = 0.5$ T was underestimated. This problem can be, however, successfully mitigated by adjusting the height of the propagating fronts [parameter B_s in (12)] with respect to B_{max}. In this way, improved predictions of the SWM were obtained [Fig. 1(c)], where $B_s = 1.9$ T at $B_{max} = 1.5$ T was used, $B_s = 1.4$ T at $B_{max} = 1.0$ T and $B_s = 1.0$ T at $B_{max} = 0.5$ T were applied, respectively. An important finding of the performed analysis is that the SWM is not limited for a certain excitation dynamics range and shape—it performs very well for arbitrary excitation waveform shapes.

Furthermore, it is very interesting to compare the predicted distributions of magnetic flux densities with respect to the

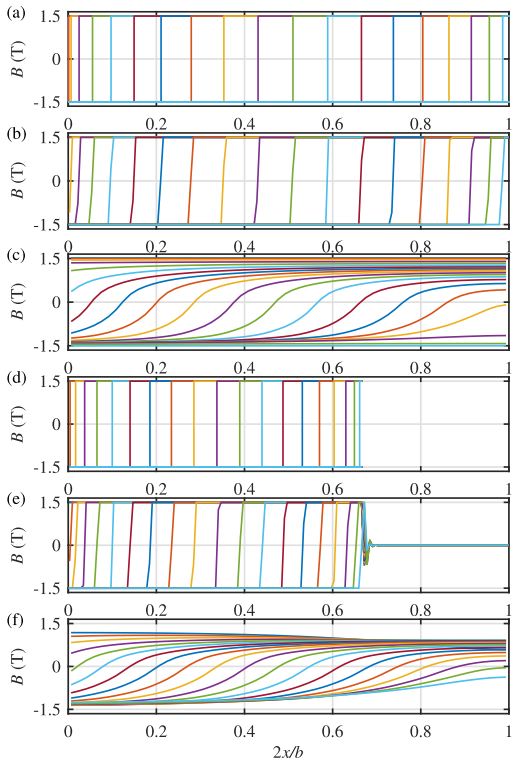

Fig. 3. Calculated wavefronts at 20 equally distributed time instants in a quarter period. (a) SWM at $B_{\max} = 1.5$ T. (b) PMD model at $B_{\max} = 1.5$ T [steplike, corresponds to Fig. 2(a)]. (c) PMD model at $B_{\max} = 1.5$ T [*M400-50A*]. (d) SWM at $B_{\max} = 1.0$ T. (e) PMD model at $B_{\max} = 1.0$ T [steplike, corresponds to Fig. 2(b)]. (f) PMD model at $B_{\max} = 1.0$ T [*M400-50A*].

depth of the SMSS at different time instants. In this way, the propagation of the wavefronts is observed. The comparison of predicted wavefronts for both the models when $B_a(t)$ decreases from 1.5 to -1.5 T and from 1 to -1 T is shown in Fig. 3(a)–(c) and (d)–(f), respectively. The wavefronts are shown at 20 equally distributed time instants in a quarter period that corresponds to Fig. 2(a) and (b). In the case of steplike magnetization curve, both the models predict similar wavefronts of negative amplitude that propagate with varying speed [in accordance with (9)] from the surface to the middle of the SMSS [Fig. 3(a) and (b) and (d) and (e)]. The wavefronts of the PMD model have limited slope due to the spatial discretization, but agree with the ideal wavefronts of the SWM very well [Fig. 3(b) and (e)].

Interesting results are obtained when analyzing wavefronts that correspond to Fig. 2(b), where $B_a(t)$ decreases from 1.0 to -1.0 T [Fig. 3(d) and (e)]. According to (9), the wavefronts of the SWM do not reach the middle of the SMSS, because $B(0) < B_s$. At first sight this seems confusing, however, the prediction of the PMD model in Fig. 3(e) validates the behavior of the wavefronts. If $B(0) < B_s$, the feedback influence of eddy currents limits the propagating wavefront to the area closer to the surface of the SMSS; hence skin effect is observed. The same effect can be observed in Fig. 2(b), where $B(t)$ in outer slices closer to the surface (slices 54 to 160) changes rapidly from $B_s(t)$ to $-B_s(t)$. In contrast to this $B(t)$ in the inner slices (slices 1 to 50) is not affected by the surface excitation at all.

Comparing the discussed wavefronts with those caused by the nonlinear magnetization curve [Fig. 3(c) and (f)], the source of the error in Fig. 1(b) is clear. The shape of the propagating wavefront has limited slope due to the limited slope of the magnetization curve. Furthermore, the shape varies with x where also the amplitude of the wavefront varies. Although these effects cannot be taken into account by use of the discussed ideal rectangular wavefront, a surprisingly good approximation can be made when the height of the propagating fronts is adjusted, as shown in Fig. 1(c).

IV. Conclusion

In this paper, the theoretical background of the simplified SWM model is presented. The presented analysis gives detailed insight into the basic fundamentals of the SWM that are discussed and validated by comparing the SWM with the solution of the 1-D diffusion phenomena predicted by the PMD model. The biggest advantage of the presented SWM model is that it is significantly simpler compared with the discretized PMD or other similar models. Despite its simplicity, SWM predicts exact solutions of the discussed problems when steplike magnetization curves are assumed and reasonably accurate predictions when real magnetization curves are assumed. The described properties make the SWM an interesting candidate for further development.

References

[1] G. Bertotti, *Hysteresis in Magnetism: For Physicists, Materials Scientists, and Engineers*, San Diego, CA, USA: Academic, 1998.
[2] M. Petrun, S. Steentjes, K. Hameyer, and D. Dolinar, "1-D lamination models for calculating the magnetization dynamics in non-oriented soft magnetic steel sheets," *IEEE Trans. Magn.*, vol. 52, no. 3, pp. 1–4, Mar. 2016.
[3] S. E. Zirka, Y. I. Moroz, P. Marketos, A. J. Moses, D. C. Jiles, and T. Matsuo, "Generalization of the classical method for calculating dynamic hysteresis loops in grain-oriented electrical steels," *IEEE Trans. Magn.*, vol. 44, no. 9, pp. 2113–2126, Sep. 2008.
[4] S. Steentjes, S. E. Zirka, Y. E. Moroz, E. Y. Moroz, and K. Hameyer, "Dynamic magnetization model of nonoriented steel sheets," *IEEE Trans. Magn.*, vol. 50, no. 4, pp. 1–4, Apr. 2014.
[5] E. Dlala, "A simplified iron loss model for laminated magnetic cores," *IEEE Trans. Magn.*, vol. 44, no. 11, pp. 3169–3172, Nov. 2008.
[6] C. Serpico, C. Visone, I. D. Mayergoyz, V. Basso, and G. Miano, "Eddy current losses in ferromagnetic laminations," *J. Appl. Phys.*, vol. 87, no. 9, p. 6923, 2000.
[7] S. Steentjes, S. E. Zirka, Y. I. Moroz, E. Y. Moroz, and K. Hameyer, "A simplified model of ferromagnetic sheets considering the magnetization dynamics utilizing the saturation wave model," *J. Appl. Phys.*, vol. 115, no. 17, p. 17D114, 2014.
[8] W. Wolman and H. Kaden, "Über die wirbelstromverzögerung magnetischer schaltvorgänge," *Zeitschrift Techn. Phys.*, vol. 13, no. 7, pp. 330–335, Jul. 1932.
[9] M. Petrun, V. Podlogar, S. Steentjes, K. Hameyer, and D. Dolinar, "A parametric magneto-dynamic model of soft magnetic steel sheets," *IEEE Trans. Magn.*, vol. 50, no. 4, pp. 1–4, Apr. 2014.
[10] M. Petrun, V. Podlogar, S. Steentjes, K. Hameyer, and D. Dolinar, "Power loss calculation using the parametric magneto-dynamic model of soft magnetic steel sheets," *IEEE Trans. Magn.*, vol. 50, no. 11, pp. 1–4, Nov. 2014.
[11] M. Petrun, S. Steentjes, K. Hameyer, J. Ritonja, and D. Dolinar, "Effects of saturation and hysteresis on magnetization dynamics: Analysis of different material models," *Compel-Int. J. Comp. Math. Electr. Electron. Eng.*, vol. 34, no. 3, pp. 710–723, 2015.
[12] S. E. Zirka *et al.*, "Dynamic magnetization models for soft ferromagnetic materials with coarse and fine domain structures," *J. Magn. Magn. Mater.*, vol. 394, pp. 229–236, Nov. 2015.